https://doi.org/10.5194/wes-2023-92
Preprint. Discussion started: 10 August 2023

eawe european academy of wind energy
Open Access WIND ENERGY SCIENCE DISCUSSIONS

Nonlinear Vibration Characteristics of Wind Turbine Blades Based on Virtual Mass Match

Aiguo Zhou[1], Jinlei Shi[1], Tao Dong[1], Yi Ma[1], Zhenhui Weng[2]

[1]School of Mechanical Engineering, Tongji University, Shanghai 200082
[2]Aeolon Technology Co., Ltd, Shanghai 200120, China

Correspondence to: *Jinlei Shi* (*shijinlei1430@163.com*)

Abstract. To analyze the nonlinear effects of the virtual masses used for load decoupling on the vibration characteristics in the biaxial fatigue test of wind turbine blades, the equivalent dynamic model of the blade-virtual masses test system is established using the Lagrange method firstly. Then, the nonlinear effects of blade amplitude and installation parameters of virtual masses on the test system are obtained by numerical methods. Moreover, the nonlinear amplitude-frequency characteristics of the test system is analyzed theoretically based on the nonlinear vibration theory. Finally, two blades over 80m are analyzed under the dynamic simulation environment. The results indicate that the resonance frequency of the test system decreases with the increase of the amplitude of the blade, presenting the nonlinear amplitude-frequency characteristics. In the case of 80m blade, the resonance frequency of the test system decreases by approximately 2%. There is also a nonlinear relation between the length of the seesaw used to install the virtual masses and the resonance frequency. The decrease of resonance frequency of the test system is more obvious with shorter seesaw, the resonance frequency decreases by up to 1.8% under certain conditions. The decrease of the resonance frequency will also reduce the area of interest for blade load verification, the blade load distribution decreases by nearly 3% in the flap-wise direction under the given operating conditions. In addition, the virtual masses will also affect the resonance characteristics and the spatial trajectory of the blade during the biaxial test.

1 Introduction

As an important component of wind turbine, the cost of blades accounts for 20% of the overall machine, so the lifetime of blades is the premise to ensure safe and stable operation of the wind turbine (Zhang et al., 2015; Liao et al., 2016). To verify the reliability of the blade under the actual operating field, the International Electrotechnical Commission (IEC) points out that the full-scale fatigue test of rotor blades is needed to be performed (IEC, 2014), which means two separate oscillations with over one million damage-equivalent loads cycles are performed at the 1st and 2nd natural frequency of the blade.

The fatigue test requires that the load in the area of interest along the blade span-wise direction matches or exceeds the design value, while keeping the exceedance as small as possible in order to avoid unrealistic failures(DNV GL AS, 2015). To satisfy the above requirements, additional masses are usually attached to the blade to tune the test load distribution which needs to be optimized by determining the optimal mass distribution.

To save testing time and to emulate the comprehensive damage along the circumference of the blade, several institutions began to study and design biaxial fatigue test (White et al., 2004; Greaves et al., 2012; Snowberg et al., 2014; Hughes et al., 1999; Liao et al., 2014;), namely to excites the blade in both directions simultaneously. Compared with the uniaxial fatigue test, the biaxial fatigue test has more complicated masses matching. Because the additional masses will affect the load distribution in both directions simultaneously, which is called as masses coupling. To solve the problem of masses coupling in the biaxial fatigue test, some test institutions introduce the concept of virtual masses.

Post et al. (2016) firstly proposed the concept of virtual masses to tune both natural frequencies independently in the two directions, and to eliminate the coupling phenomenon of test bending moments during biaxial test. Melcher et al. (2020、2021) used elastic elements to adjust blade stiffness, and optimized biaxial fatigue test parameters based on virtual masses and elastic elements. Zhang et al. (2020) and Lu et al. (2022) carried out research on biaxial load matching and design using virtual masses.

https://doi.org/10.5194/wes-2023-92
Preprint. Discussion started: 10 August 2023

The above research work regards the virtual masses used for masses decoupling as translational motion, which is difficult to apply to the actual test field. Because it requires large equipment and is difficult to apply to the test condition of large blade vibration. Therefore, IWES conducted further research, designed a device to convert virtual masses from translation to rotation, and applied it to the biaxial fatigue test which has a frequency ratio of 1:1. Further, the feasibility of the biaxial decoupling test of the bending moment was verified by the comparison of simulation and experiment results (Melcher et al., 2020; Falko et al., 2020; Castro et al.,2021). In fact, in the view of the motion characteristics, the inertia force generated by rotating virtual masses is different from that generated by translational virtual masses.

This work establishes the dynamic model of the blade-virtual masses test system and analyses the nonlinear amplitude-frequency characteristics of the test system. The aim is to further analyze the effect of rotating virtual masses on the blade test system, and to reveal the vibration mechanism of the blade-virtual masses test system to provide a more rigorous theoretical basis for the biaxial load matching theory of the blade. Moreover, two blades over 80m were simulated to verify the nonlinear vibration characteristics of the test system and evaluate the effect of installation parameters of virtual masses on blade test load distribution, such as the length of the seesaw.

2 Blade-virtual masses equivalent dynamic model

The additional masses can change the modal characteristics of the testing system to adjust the test load distribution of the blade, which is essentially bending moment caused by the inertia force brought by the reciprocating motion of the self-weight and additional masses. In the common fatigue test system, the additional masses are directly attached to the blade. When the additional masses are determined, the modal characteristics of the testing system are basically determined, as shown in Fig. 1 (a). This means that, without considering the air damping, the resonant frequency of the system remains unchanged.

In the biaxial fatigue test, the additional mass decouples the biaxial load by seesaw, and the additional mass is called virtual mass, as shown in Fig. 1 (b). In this installation condition, the inertia force generated by the virtual mass only acts in the direction of an individual blade mode. The mechanism for mounting the virtual mass consists of a push rod and a seesaw. The push rod, blade fixture, and seesaw are connected through a universal joint, and the seesaw can rotate around the center position. Masses are located at both ends of the seesaw to offset each other's gravity. However, due to the motion characteristics of the virtual mass mechanism, the motion of the virtual mass cannot be perfectly synchronized with the blade motion. Therefore, the inertia force generated by the rotation of the virtual mass differs from the inertia force generated by the traditional tuning masses. To precisely evaluate the specific impacts of virtual mass rotation on the blade test system, it is necessary to establish a corresponding theoretical model for comprehensive analysis.

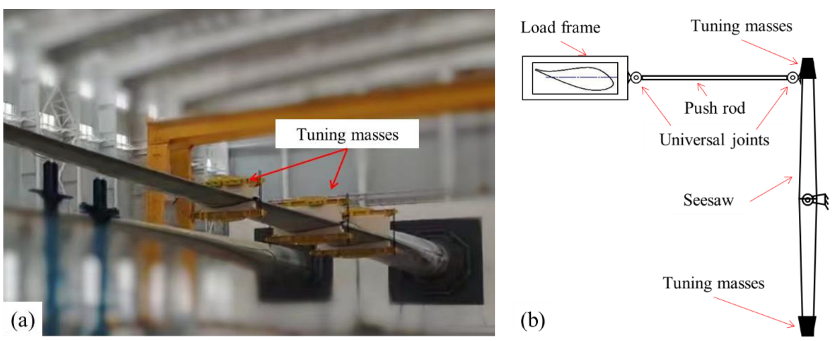

Figure 1: Masses match of blade fatigue test: (a) traditional tuning masses setup (b) virtual masses setup.

2.1 Model using the Lagrange method

The aim of virtual masses is to decouple the test load in the biaxial fatigue test. Essentially, the motion of the virtual mass generates an inertial force that is transmitted to the blades through push rods, thereby adjusting the load distribution in the

https://doi.org/10.5194/wes-2023-92
Preprint. Discussion started: 10 August 2023

main vibration direction. To more intuitively analyze the impact of virtual mass on the blade test system, taking the example of blade edge-wise direction test, the blade model is simplified as shown in Fig. 2. Moreover, the inertial force of the virtual masses also affects the flap-wise direction of the blade. However, since the frequency of the inertial force is close to the first order modal frequency in edge-wise direction, the perturbation to the flap-wise direction is relatively small. Therefore, only the influence of virtual mass on the vibration characteristics in the main testing direction needs to be considered during the uniaxial test.

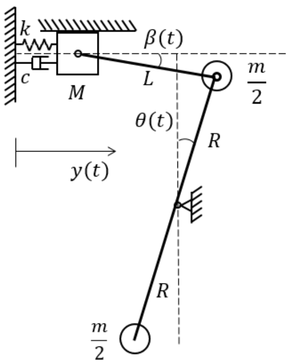

Figure2: Virtual masses setup for blade fatigue test.

$$\frac{d}{dt}\left(\frac{\partial T}{\partial \dot{q}_j}\right)-\frac{\partial T}{\partial q_j}+\frac{\partial V}{\partial q_j}+\frac{\partial D}{\partial \dot{q}_j}=Q_j, j=1,2,\cdots,n \tag{1}$$

Where: T- kinetic energy; V- potential energy; D- dissipated energy; q_j- generalized coordinate; $\dot{q}_j$ - generalized velocity; Q_j - generalized force.

By selecting the generalized coordinate $q=y$, and based on the motion relationship in Fig. 2, the displacement and velocity relationships of the test system can be obtained:

$$\begin{cases} y+L\cos\beta-R\sin\theta=L \\ L\sin\beta+R\cos\theta=R \end{cases} \tag{2}$$

$$\begin{cases} \dot{y}-L\dot{\beta}\sin\beta-R\dot{\theta}\cos\theta=0 \\ L\dot{\beta}\cos\beta-R\theta\sin\theta=0 \end{cases} \tag{3}$$

T, V and D can be calculated as

$$T=\frac{1}{2}M\dot{y}^2+\frac{1}{2}mR^2\dot{\theta}^2=\frac{1}{2}M\dot{y}^2+\frac{1}{2}m\dot{y}^2\frac{\cos^2\beta}{\cos^2(\theta-\beta)} \tag{4}$$

$$V=\frac{1}{2}ky^2 \tag{5}$$

$$D=\frac{1}{2}c\dot{y}^2 \tag{6}$$

Where: L - the length of the push rod; R - the radius of the seesaw; β - the angle between the push rod and the horizontal direction; θ - the angle between the seesaw and the vertical direction; M - blade equivalent mass; m – virtual masses; k - blade equivalent stiffness; c - blade equivalent damping.

According to Eqs. (2) and Eqs. (3), the relevant terms in Eqs. (1) are obtained as

https://doi.org/10.5194/wes-2023-92
Preprint. Discussion started: 10 August 2023

$$\begin{cases} \frac{d}{dt}\left(\frac{\partial T}{\partial \dot{y}}\right) = M\ddot{y} + m\ddot{y}\frac{\cos^2\beta}{\cos^2(\theta-\beta)} + m\dot{y}\frac{d}{dt}\left[\frac{\cos^2\beta}{\cos^2(\theta-\beta)}\right] \\ \frac{\partial T}{\partial y} = \frac{1}{2}m\dot{y}^2\frac{\partial}{\partial y}\left[\frac{\cos^2\beta}{\cos^2(\theta-\beta)}\right] \\ \frac{\partial V}{\partial y} = ky \\ \frac{\partial \Psi}{\partial \dot{y}} = c\dot{y} \\ Q(t) = F(t) \end{cases} \tag{7}$$

Then, the dynamic differential equation of test system is

$$\left\{M + m\frac{\cos^2\beta}{\cos^2(\theta-\beta)}\right\}\ddot{y} + c\dot{y} + ky + \frac{m\dot{y}^2\cos\beta}{\cos^4(\theta-\beta)}\left[\frac{\cos^2\beta\sin(\theta-\beta)}{R} - \frac{\sin^2\theta}{L}\right] = F(t) \tag{8}$$

Where:

$$\sin\theta = \frac{L+y}{R} - \frac{L\left(R\sqrt{-(y^2+2Ly-2LR)(y^2+2Ly+2LR)}+y^3+2L^3+4L^2y+3Ly^2\right)}{2R(L^3+2L^2y+LR^2+Ly^2)}$$

$$\cos\theta = \frac{L(L+y)[R\sqrt{-(y^2+2Ly-2LR)(y^2+2Ly+2LR)}+2L^3+y^3+3Ly^2+4L^2y]}{2R^2(L^3+2L^2y+LR^2+Ly^2)} - \frac{2L^2+2Ly-2R^2+y^2}{2R^2}$$

$$\sin\beta = \frac{2L^2+2Ly+y^2}{2LR} - \frac{(L+y)[R\sqrt{-(y^2+2Ly-2LR)(y^2+2Ly+2LR)}+2L^3+y^3+3Ly^2+4L^2y]}{2R(L^3+2L^2y+LR^2+Ly^2)}$$

$$\cos\beta = \frac{R\sqrt{-(y^2+2Ly-2LR)(y^2+2Ly+2LR)}+2L^3+y^3+3Ly^2+4L^2y}{2(L^3+2L^2y+LR^2+Ly^2)}$$

According to Eqs. (8), it can be seen that rotation of virtual masses introduces nonlinear terms to the test system, and both the angle θ and β are nonlinear functions of the blade response y. Due to the complexity of the dynamic equation, it is difficult to obtain the corresponding analytical expression. Therefore, the numerical analysis methods are used to solve the equation. As mentioned previously, the nonlinear factors that affect the characteristics of the test system mainly come from installation parameters (pushrod length and seesaw radius) and blade response. The design length of the push rod typically remains unchanged due to space limitations at the test site. However, the seesaw radius offers greater design flexibility. Thus, the primary focus is on evaluating the impact of the seesaw radius R and blade response y on the vibration characteristics of the blade. To illustrate this, numerical analysis is performed on the equivalent model of an 80m blade to examine the impact of blade amplitude on the resonance frequency of the testing system. This investigation is carried out by considering different virtual masses and radius of the seesaw, as demonstrated in Fig. 3.

Figure 3 (a) shows that the resonance frequency of the test system decreases nonlinearly with an increase in blade amplitude and virtual masses m further determines the rate of decrease in resonance frequency. The equivalent stiffness k has the ability to alter the natural frequency of the test system. However, it can be seen Fig. 3 (b) that k cannot change the rate of decrease in resonance frequency with other parameters unchanged, which indicates that the equivalent stiffness is not a nonlinear factor affecting the vibration characteristics of the testing system. Fig. 3 (a) shows that the radius of the seesaw will also affect the nonlinear amplitude-frequency characteristics of the test system and the rate of decrease in resonance frequency.

https://doi.org/10.5194/wes-2023-92
Preprint. Discussion started: 10 August 2023

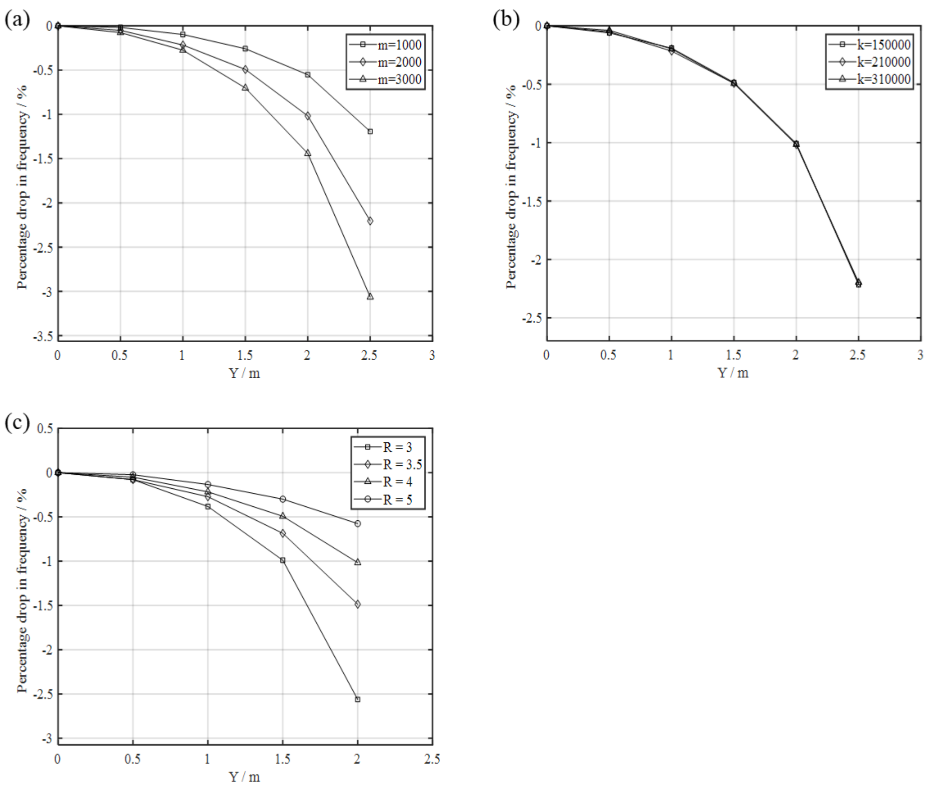

Figure 3: The relationship between resonant frequency and amplitude at different parameters: (a) $M = 14000kg$; $k = 210000N/m$; $L = 4m$; $R = 4m$ (b) $M = 14000kg$; $m = 2000kg$; $L = 4m$; $R = 4m$ (c) $M = 14000kg$; $k = 210000N/m$; $m = 2000kg$; $L = 4m$.

2.2 Analysis of amplitude-frequency characteristics of the model

As previously mentioned, both virtual mass and traditional additional masses adjust the load distribution of the measured blade by changing the modal characteristics of the blade through the inertial force originated from the blade movement. However, due to the motion of the virtual masses mechanism, a distinct inertial force from that of traditional additional masses, which contributes to the nonlinearity of the test system. The dynamic differential equations of the blade-virtual masses test system, established through the Lagrange method, are highly complex and can only be resolved numerically to derive the correlations among the relevant parameters and the resonance frequency of the test system. To quantitatively analyze the nonlinear amplitude-frequency characteristics of the test system, it is necessary to construct a theoretical model of the test system based on nonlinear dynamics. According to linear vibration theory, the factors that primarily influence the inherent characteristics of a linear system are the inertial force term and the elastic force term. In fact, the inherent characteristics of the blade-virtual masses test system are primarily determined by the inertial force term associated with the introduction of virtual mass and the response of the blade Thus, the weakly nonlinear dynamic equation of the blade-virtual mass test system in Fig. 2 can be approximated as:

$$(M+m)f(y)\ddot{y} + c\dot{y} + ky = F_0 \cos(\omega t + \theta) \tag{9}$$

Where: $f(y) = 1 + \varepsilon_1 y + \varepsilon_2 y^2 + \varepsilon_3 y^3 + \varepsilon_4 y^4$; $c = 2\zeta(M+m)\omega_n$; $k = (M+m)\omega_n^2$; $F_0 = Bk$; ε_1、ε_2、ε_3、ε_4 - Small parameters related to M、m、L and R; ζ - Damping ratio; ω_n - Natural frequency; ω - Excitation frequency; θ - Phase difference between steady-state response and excitation.

Ignoring the small parameters, Eqs. (9) is transformed into the vibration equation of a linear system. This means that the linear system is derived from the original nonlinear system. To quantitatively analyze the modal characteristics of the test

https://doi.org/10.5194/wes-2023-92
Preprint. Discussion started: 10 August 2023

system, the approximate analytical method can be employed by considering the nonlinear factor as a perturbation to the linear system, yielding an approximate analytical solution for the nonlinear system. Among various approximate analytical methods, the harmonic balance method is particularly notable due to its clear conceptual foundation. It expands both the excitation term and the solution of the equation into a Fourier series. From a physical perspective, the coefficients of the harmonic terms of the same order at both ends of the dynamic equation must be equal to maintain a balance between the excitation and inertia forces.

For the blade-virtual masses testing system, it is assumed that its steady-state response is still periodic, but the resonance frequency is different from the natural frequency of the derived system. The basic solution is expanded into the Fourier series of the excitation frequency and the fundamental component is retained. The response of the system as Eq. (10) indicates.

$$y(t) = Y_0 \cos(\omega t) \tag{10}$$

Where: Y_0 - Amplitude of blade steady-state response.

By substituting Eq. (10) into Eq. (9) and applying the triangle transform and harmonic balance to eliminate the phase difference θ to achieve the relationship between the amplitude and frequency of the test system, as Eq. (11) indicates.

$$\left[1 - s^2\left(1 + \frac{3}{4}\varepsilon_2 {Y_0}^2 + \frac{10}{16}\varepsilon_4 {Y_0}^4\right)\right]^2 + (2\zeta s)^2 = \left(\frac{B}{Y_0}\right)^2 \tag{11}$$

Where: $s = \omega/\omega_n$.

According to Eq. (11), The amplitude-frequency and phase-frequency characteristics of the nonlinear system can be obtained, as Eq. (12) indicates.

$$\begin{cases} \dfrac{Y_0}{B} = \dfrac{1}{\sqrt{\left[1-s^2\left(1+\frac{3}{4}\varepsilon_2 {Y_0}^2+\frac{10}{16}\varepsilon_4 {Y_0}^4\right)\right]^2+(2\zeta s)^2}} \\ \theta = \arctan\left[\dfrac{2\zeta s}{1-s^2\left(1+\frac{3}{4}\varepsilon_2 {Y_0}^2+\frac{10}{16}\varepsilon_4 {Y_0}^4\right)}\right] \end{cases} \tag{12}$$

When $\varepsilon_2 = \varepsilon_4 = 0$, Eq. (12) describes the amplitude-frequency characteristics of a linear system, as shown in Fig. 4. When the small parameters are non-zero, the amplitude-frequency characteristic curve of the nonlinear system is depicted in Fig. 5. Similar to forced vibrations in linear systems, nonlinear systems also exhibit similar amplitude-frequency characteristic curves. However, the backbone of the support curve clusters is not straight but inclined. This backbone curve represents the variation of the free vibration frequency of the nonlinear system with respect to the amplitude when there is no external excitation. By setting B = 1 and ζ = 0 in Eq. (11), the equation for this backbone curve can be obtained, as Eq. (13) indicates.

$$\omega^2 = \frac{\omega_n^2}{\left(1+\frac{3}{4}\varepsilon_2 {Y_0}^2+\frac{10}{16}\varepsilon_4 {Y_0}^4\right)} \tag{13}$$

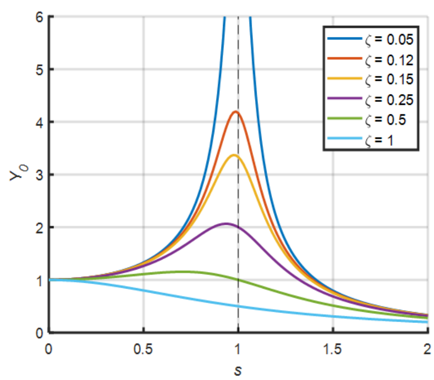

Figure 4: Amplitude-frequency characteristic curve of a linear system

Eq. (13) shows that the resonance frequency of the blade-virtual masses test system decreases with the increase of the

https://doi.org/10.5194/wes-2023-92
Preprint. Discussion started: 10 August 2023

amplitude of the blade and there exists the nonlinear relationship between the square of the frequency ratio and the amplitude. Figure 5 shows that the small parameters in the inertial force term will affect the frequency of free vibration. As these parameters decrease, the amplitude-frequency characteristic curve of a nonlinear system approaches that of a linear system, and the backbone curve approaches a value close to 1.

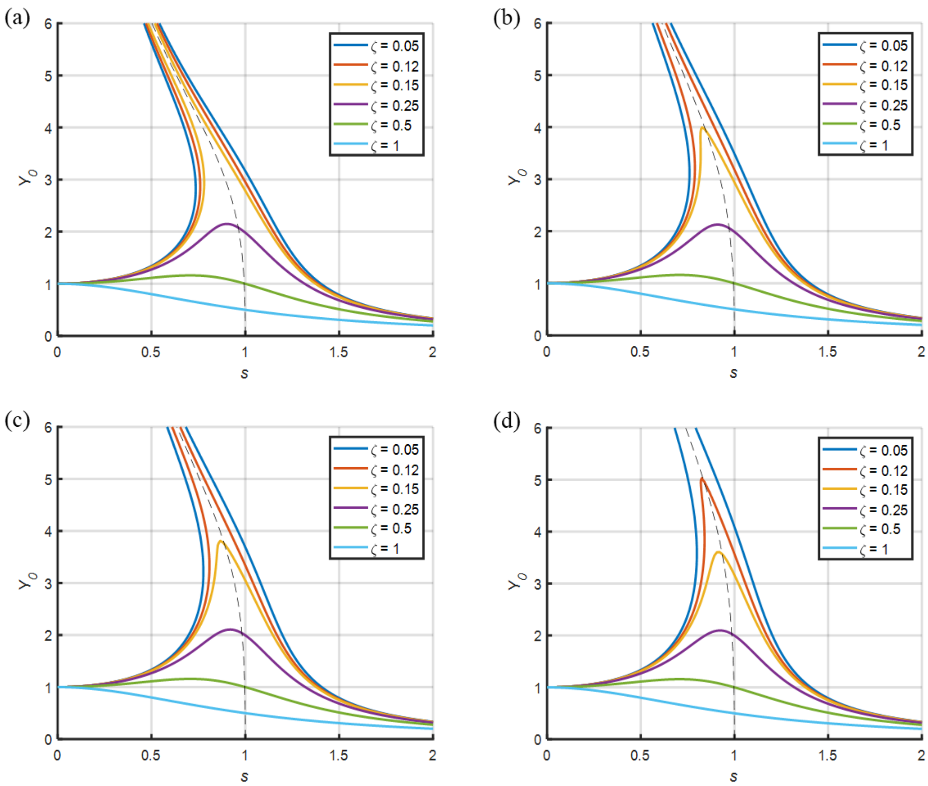

Figure 5: Amplitude-frequency characteristic and the backbone (represented by the black dashed line) of the blade-virtual masses testing system: (a) $B = 1$、$\frac{3}{4}\varepsilon_2 = 0.01$、$\frac{10}{16}\varepsilon_4 = 0.002$ (b) $B = 1$、$\frac{3}{4}\varepsilon_2 = 0.01$、$\frac{10}{16}\varepsilon_4 = 0.001$ (c) $B = 1$、$\frac{3}{4}\varepsilon_2 = 0.005$、$\frac{10}{16}\varepsilon_4 = 0.001$ (d) $B = 1$、$\frac{3}{4}\varepsilon_2 = 0.005$、$\frac{10}{16}\varepsilon_4 = 0.0005$.

3 Dynamic simulation analysis

To validate the nonlinear characteristics of the blade-virtual mass test system that has been established, it is necessary to utilize simulation software to create a realistic blade model for analysis. Based on the sectional properties and tuning masses of the blade, motion analysis software can be employed for modeling and analyzing the blade-virtual masses system. The simulation software can perform modal analysis and harmonic analysis to obtain the changing characteristic of the testing system under various operating conditions.

3.1 Simulation Modeling

To verify that the simplified equivalent theoretical model can reflect the characteristics of actual test system, the simulation model is established in software. The root of the blade was set as a fixed constraint to simulate the cantilever beam condition similar to when the blade is mounted on the test rig. The equivalent damping ratio of the blade changes during vibration, resulting in a change in the resonance frequency of the test system. In order to accurately assess the influence of virtual mass on the characteristics of the testing system, aerodynamic damping is not considered in the simulation model. The blade model

https://doi.org/10.5194/wes-2023-92
Preprint. Discussion started: 10 August 2023

was built in the simulation software based on the parameters mentioned above, as shown in Fig. 6(a).

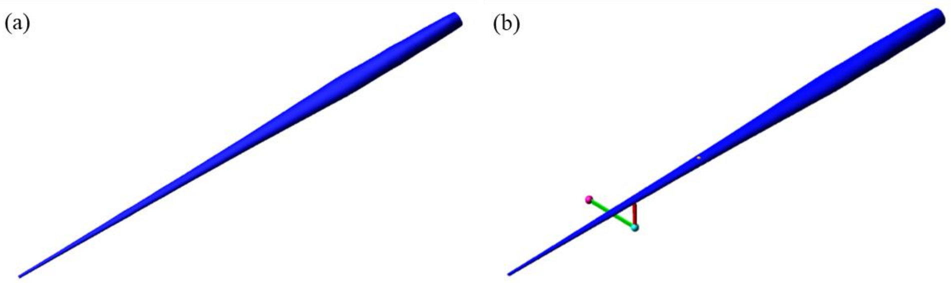

Figure 6: Dynamics simulation model of test system: (a) The blade simulation model (b) The blade-virtual masses simulation model(flap-wise)

3.2 Model validity verification

To ensure the applicability of the model, modal analysis is carried out and compared with the transfer-matrix method (TMM) and the test data, taking the calculation of the flap-wise direction as an example, as shown in Table 1. It can be seen that the simulation model of the test system exhibits a high level of accuracy, with an error in the modal frequency of less than 4%.

Table1. Blade modal analysis in flap-wise direction

Flap-wise	84m		94m		102m	
Method	1st modal frequency [Hz]	Error [%]	1st modal frequency [Hz]	Error [%]	1st modal frequency [Hz]	Error [%]
Test	0.394	-	0.365	-	0.434	-
TMM	0.397	+0.7	0.349	-4.38	0.420	-3.22
Simulation	0.404	+2.54	0.377	+3.29	0.421	-2.99

3.3 Simulation setup

With the purpose of demonstrating the nonlinear effect of rotating virtual masses on the testing system, it is necessary to add virtual masses based on the blade model, as shown in Fig.6(b). The values of the additional masses are shown in Table 2 and the section properties of the blades are shown in Fig. 7. Virtual mass elements are added at 62% and 49% of the 84m blade length in the flap-wise and edge-wise directions respectively. Similarly, virtual mass elements are added at 63% and 52% of the 94m blade length in the flap-wise and edge-wise directions respectively (marked in black italics in Table 2). The constraints for the seesaw, push rod, and virtual masses are set according to Fig. 1, where the rotation center of the seesaw is set as the revolute pair and the seesaw and push rod are set as the rigid light rod. To evaluate and verify the effects of virtual masses installation parameters and blade response on the vibration characteristics of the testing system, not only the effects of radius of the seesaw and blade response on the resonance frequency, but also the effects of radius of the seesaw on the load distribution of the blade with similar amplitude are analyzed through simulation.

Table2. Blade additional masses of 84m and 94m blade

84m			94m		
Location	Flap-wise masses [kg]	Edge-wise masses [kg]	Location	Flap-wise masses [kg]	Edge-wise masses [kg]
26%		2835	42%	3000	3000
36%		3147	52%		***4075***
49%	6120	***4075***	63%	***1116***	
62%	***1117***				

https://doi.org/10.5194/wes-2023-92
Preprint. Discussion started: 10 August 2023

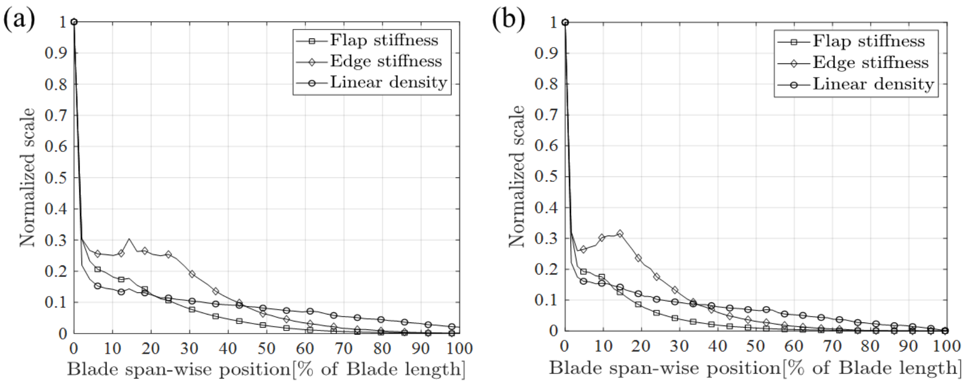

Figure 7: Section properties of the blade: (a) 84m blade (b) 94m blade

As the foundation for other dynamics analysis, modal analysis is used to determine the modal characteristics of structures. Regarding the weakness of modal analysis function in the software, which cannot consider the effects of the response on the modal characteristics of the system, it is necessary to take further sweep-frequency analysis to obtain the resonance characteristics of the system. The sweep-frequency analysis is to apply a series of harmonic excitation with different frequencies to the system to analyze its response spectrum.

4 Results

According to the backbone in the amplitude-frequency characteristic curve of the blade-virtual masses test system, when the operation condition determined, the square of the resonance frequency and the blade amplitude satisfy the relationship in Eqs. (13). Thus, correlated simulation results are fitted using relevant functions to verify the relationship.

4.1 Effects of amplitude on resonance frequency

Set R = 4m and L = 4m and investigate the variation of the resonance frequency of test system under different amplitudes. Sweep-frequency analysis is performed on the 84m and 94m blades in flap-wise and edge-wise directions respectively to obtain the resonance frequencies of the test system under different steady-state amplitudes while the results are fitted according to Eqs. (13), as shown in Fig. 8. When amplitude of the blade is small, the percentage drop in resonance frequency is small. When amplitude of the blade is large, the resonance frequency presents nonlinear rapid decline. When the blade amplitude in flap-wise direction reaches 2.6m, the resonance frequency of the 84m and 94m blades decreases by approximately 2.0%; When the blade amplitude in edge-wise direction reaches 2.2m, the resonance frequency of the 84m and 94m blades decreases by approximately 1.1%.

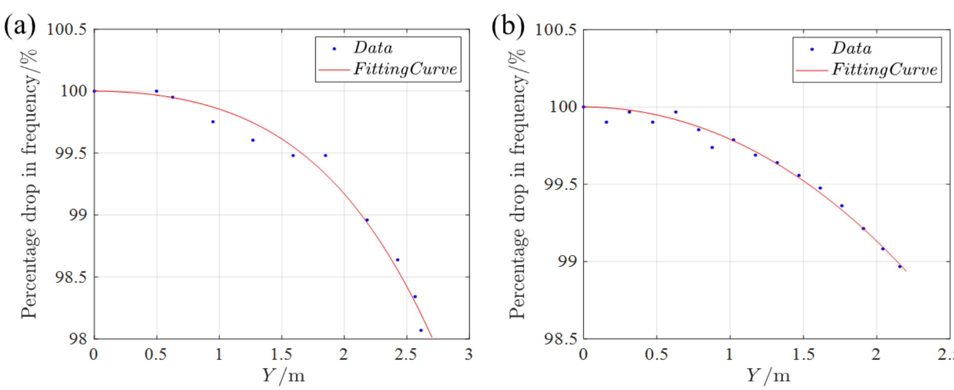

https://doi.org/10.5194/wes-2023-92
Preprint. Discussion started: 10 August 2023

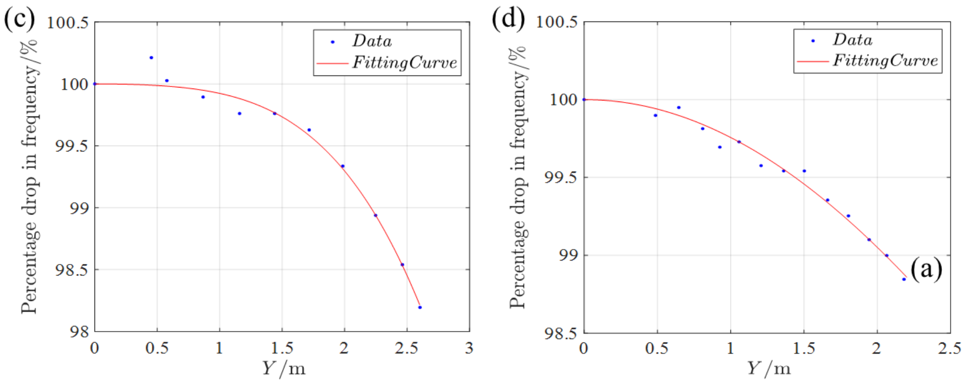

Figure 8: Relationship between amplitude and percentage drop in resonance frequency: (a) 84m blade in flap-wise direction (b) 84m blade in edge-wise direction (c) 94m blade in flap-wise direction (d) 94m blade in edge-wise direction

4.2 Effects of radius of the seesaw on resonance frequency and load distribution

Considering the experimental setup, the blade amplitude in flap-wise direction is set to be about *Y*=2m and the length of the push rod is *L*=4m; the blade amplitude in edge-wise direction is about *Y*=1m and the length of the push rod is *L*=4m. The sweep-frequency analysis of the 84m and 94m blades in flap-wise and edge-wise directions is carried out respectively to obtain the resonance frequency of the test system. According to Eqs. (13), appropriate function (Eqs. (14)) is selected to fit the results, as shown in Fig. 9. Considering equations (13) and (14), the small parameters encompass the influence of radius of the seesaw, which can be approximated by an exponential function. A larger radius of the seesaw results in a smaller decrease in the resonance frequency. Conversely, when the rotation radius of the seesaw is small, the resonance frequency experiences a rapid and nonlinear decrease. With R = 3m, the drop in the resonance frequency of the 84m and 94m blades is approximately 1.6% in the flap-wise direction. Likewise, with R = 2m, the drop in the resonance frequency is approximately 1.1% in the edge-wise direction.

$$\omega^2 = \frac{\omega_n^2}{(1+ae^{-bR})} \tag{14}$$

Where: a、b - parameters in exponential function.

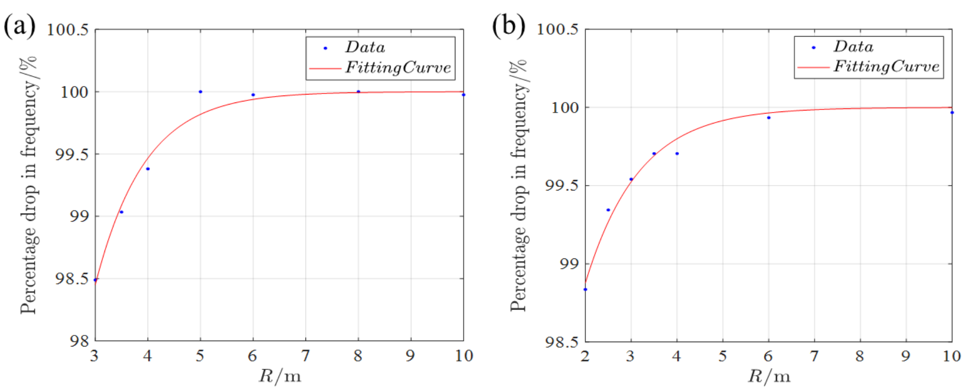

https://doi.org/10.5194/wes-2023-92
Preprint. Discussion started: 10 August 2023

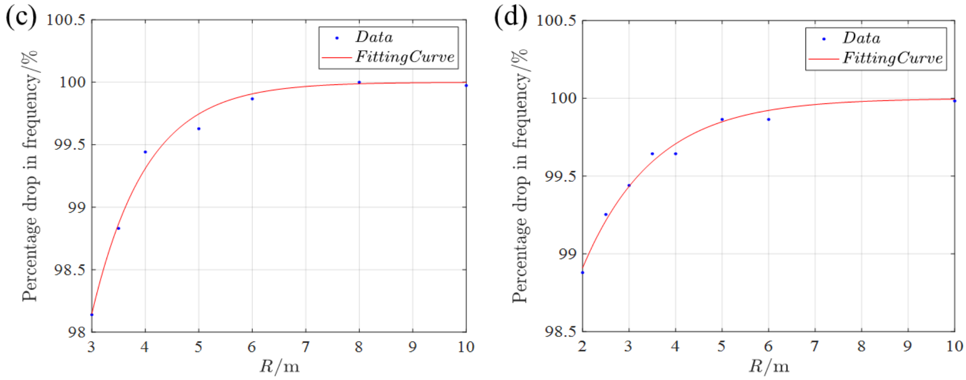

Figure 9: Relationship between radius of the seesaw and percentage drop in resonance frequency: (a) 84m blade in flap-wise direction (b) 84m blade in edge-wise direction (c) 94m blade in flap-wise direction (d) 94m blade in edge-wise direction

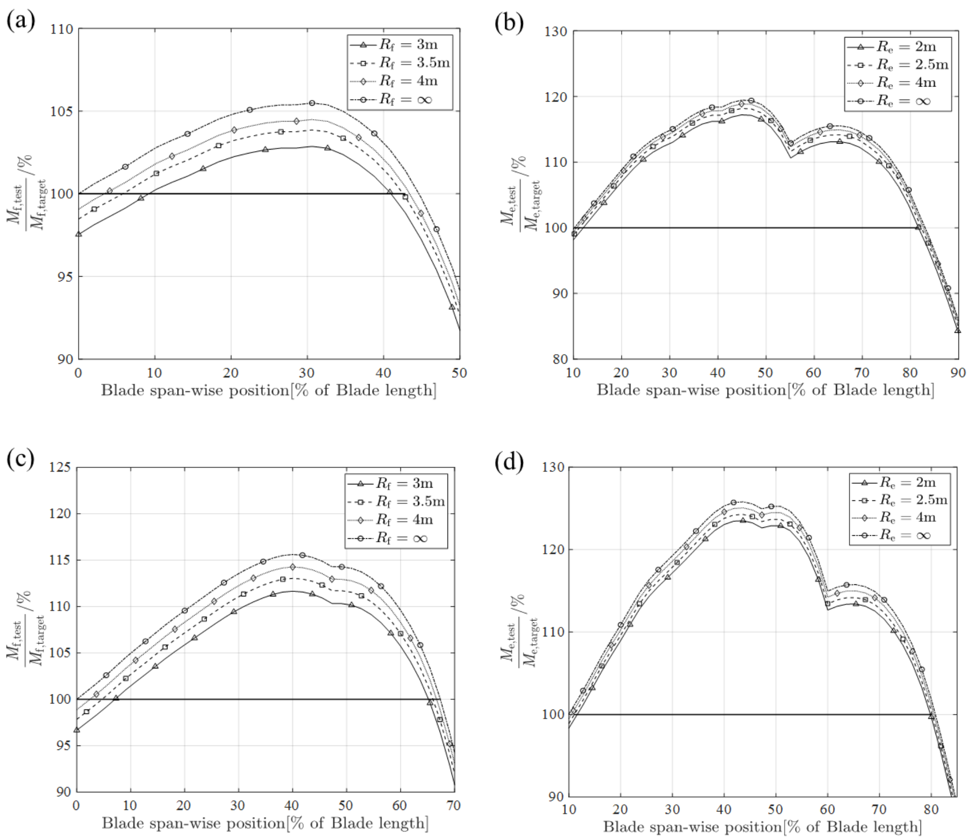

Figure 10: Relationship between radius of the seesaw and blade load distribution: (a) 84m blade in flap-wise direction (b) 84m blade in edge-wise direction (c) 94m blade in flap-wise direction (d) 94m blade in edge-wise direction

The radius of the seesaw influences the characteristics of the testing system and alters the distribution of blade loads, as shown in Fig. 10. In the case of $R = \infty$, the virtual masses shift from rotation to translation, effectively simulating additional masses that are directly fixed onto the blade. As R decreases, the amplitude of blade loads reduces rapidly. Consequently, there is an approximate 3% decrease in the overall load distribution in the flap-wise direction, resulting in a reduction in the

https://doi.org/10.5194/wes-2023-92
Preprint. Discussion started: 10 August 2023

eawe european academy of wind energy
Open Access WIND ENERGY SCIENCE DISCUSSIONS

area of interest. Given the roughly similar amplitudes, lower resonance frequencies result in reduced inertial loads on the blade. Therefore, compensatory measures such as increasing the excitation level are necessary during the actual test. However, this requires more powerful excitation equipment.

4.3 Effects of virtual masses on biaxial test

Virtual masses will affect the resonance characteristics and load distribution in both flap-wise and edge-wise directions. In the biaxial fatigue test, the coupling of vibrations in both directions further exacerbates the nonlinearity of the test system. Taking 94m blade as an example, virtual masses are applied in both flap-wise and edge-wise directions. Modal analysis and frequency sweep analysis are used to obtain the frequencies at which specific excitations are applied to the test system. The parameters are shown in Table 3, with R = 4m and L = 4m. The spatial coupling trajectory of the blade can be obtained, as shown in Fig. 11. The results show that the resonance frequencies decrease compared to uniaxial test, especially in the flap-wise direction, due to the influence of the virtual masses in both vibration directions. This is because the flap-wise direction has a larger amplitude, and the inertial forces generated by the virtual masses in the edge-wise direction produce more significant inertial component forces to the flap-wise direction. Additionally, if do not consider the influence of the blade's structural twist. It can be seen from Fig.11 that the envelope of the blade's spatial trajectory is not a regular quadrilateral, which poses new challenges for adjusting the biaxial load distribution and damage assessment.

Table3. Biaxial excitation parameters of 94m

	Virtual masses and exciting point		Modal analysis		Sweep-frequency analysis	
	Position [% of Blade length]	Force [N]	Natural frequency [Hz]	Amplitude at 63% position [m]	Resonance frequency [Hz]	Amplitude at 63% position [m]
Flap-wise	63%	3800	0.377	1.685	0.372	1.893
Edge-wise	52%	7000	0.589	1.292	0.586	1.402

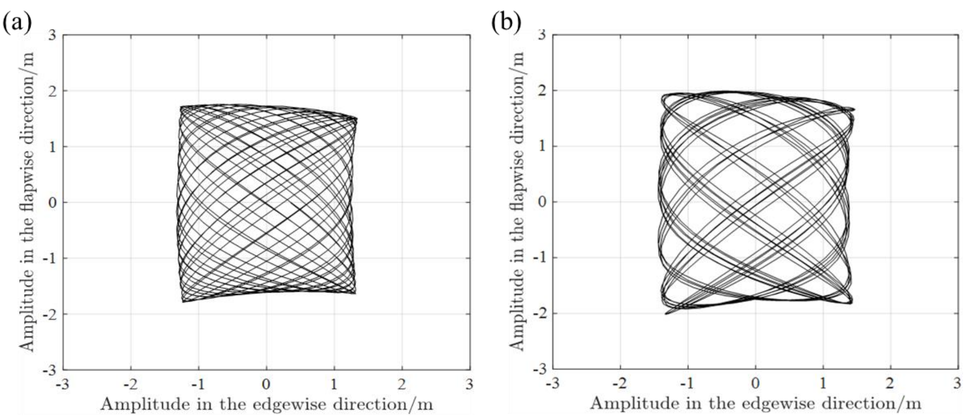

Figure 11: Biaxial trajectory of blade-virtual masses test system with same exciting force: (a) Natural frequency excitation (b) Resonance frequency excitation

5 Conclusion

This paper explores the effect of virtual masses device applied to blade biaxial fatigue test on the response characteristics of the test system. Different from the additional masses directly installed on the blade, the nonlinearity of the test system originates from kinematics of the virtual masses. Based on the analysis above, the main conclusions are shown as follows:

https://doi.org/10.5194/wes-2023-92
Preprint. Discussion started: 10 August 2023

1. The blade-virtual masses test system shows nonlinear amplitude-frequency characteristics. The square of the resonance frequency is inversely proportional to the polynomial steady-state response of the system. In the case of 80m blade, the resonance frequency of the test system decreases by approximately 2% when amplitude is 2.6m during flap-wise vibration.

2. The radius of the seesaw will also affect the vibration characteristics of the test system. The shorter the radius of the seesaw, the stronger the nonlinear effects on the test system. When the blade flap amplitude is 2m and the radius is 3m, the resonance frequency decreases by up to 1.8%. Due to the limited amplitude in the edge-wise direction, the radius of the seesaw has minimal impact on the resonance frequency.

3. The rotation radius of the seesaw will also affect the load distribution of the blade. Shortening the radius will reduce the amplitude of blade load and the verification area of interest. The blade load distribution decreases by nearly 3% in the flap-wise direction under the given operating conditions.

4. When subjected to both large amplitude and short radius of the seesaw, the resonance frequency will decrease more significantly. It is important and necessary to consider the size and strength of the push rod and seesaw during practical application. In addition to the influence on the resonance frequency and load distribution, the size and strength of the push rod and seesaw also limit the maximum amplitude of the blade and the service life of the mechanism.

References

[1] Zhang, L. A. and Huang, X. M.: Study of wind turbine blade vibration characteristics under single point fatigue load driven. Acta Energiae Solaris Sinica, 36(05): 1112-1116, https://doi.org/10.3969/j.issn.0254-0096.2015.05.013, 2015.

[2] Liao, G. H. and Wu, J. Z.: Wind turbine blade resonance fatigue loading system and experiment. Acta Energiae Solaris Sinica, 37(11): 2785-2791, https://doi.org/10.19912/j.0254-0096.2016.11.009, 2016.

[3] IEC: IEC 61400-23 – Wind Turbines Part 23: Full-scale Structural Testing of Rotor Blades, International Electrotechnical Commission, Geneva, Switzerland, 2014.

[4] DNV GL AS: DNVGL-ST-0376 – Rotor blades for wind turbines, available at: https://rules.dnvgl.com/docs/pdf/DNVGL/ST/2015-12/DNVGL-ST-0376.pdf (last access: 7 June 2019), 2015.

[5] White, D.: New method for dual-axis fatigue testing of large wind turbine blades using resonance excitation and spectral loading, Tech. rep., National Renewable Energy Lab., Golden, CO, USA, https://doi.org/10.2172/15007390, 2004.

[6] Greaves, P. R., Dominy, R. G., Ingram, G. L., Long, H., and Court, R.: Evaluation of dual-axis fatigue testing of large wind turbine blades, P. I. Mech. Eng. C-J. Mec., 226, 1693–1704, https://doi.org/10.1177/0954406211428013, 2012.

[7] Snowberg, D., Dana, S., Hughes, S., and Berling, P.: Implementation of a Biaxial Resonant Fatigue Test Method on a Large Wind Turbine Blade, Tech. rep., National Renewable Energy Laboratory, Golden, CO, USA, https://doi.org/10.2172/1155105, 2014.

[8] Hughes, S., Musial, W. D., and Stensland, T.: Implementation of a Two-Axis Servo-Hydraulic System for Full-Scale Fatigue Testing of Wind Turbine Blades, Tech. rep., National Renewable Energy Laboratory, Golden, CO, USA, https://www.osti.gov/servlets/purl/12200, 1999.

[9] Liao, G. H. and Wu, J. Z.: Vibration Analysis of a Dual-axial Fatigue Loading System for Wind Turbine's Blades Test. NOISE AND VIBRATION CONTROL, 34(05): 114-116, https://doi.org/10.3969/j.issn.1006-1335.2014.05.026, 2014.

[10] Post, N. and Bürkner, F.: Fatigue Test Design: Scenarios for Biaxial Fatigue Testing of a 60-Meter Wind Turbine Blade, Tech. rep., National Renewable Energy Laboratory, Golden, CO, USA, https://doi.org/10.2172/1271941, 2016.

[11] Melcher, D., Bätge, M., and Neßlinger, S.: A novel rotor blade fatigue test setup with elliptical biaxial resonant excitation, Wind Energ. Sci, 5(2): 675-684, https://doi.org/10.5194/wes-5-675-2020, 2020.

[12] Melcher, D., Petersen, E., and Neßlinger, S.: Off-axis loading in rotor blade fatigue tests with elliptical biaxial resonant excitation, J. Phys. Conf. Ser, 1618(5): 052010, https://doi.org/10.1088/1742-6596/1618/5/052010, 2020.

[13] Lu, L., Zhu, M., and Wu, H.: A Review and Case Analysis on Biaxial Synchronous Loading Technology and Fast Moment-Matching Methods for Fatigue Tests of Wind Turbine Blades. ENERGIES, 15(13) :4881, https://doi.org/10.3390/en15134881, 2022.

[14] Zhang, J. B., Shi, K. Z., and Zhang, C. Y.: Improving accuracy of dual-axial resonance fatigue testing for wind turbine

blades by using predicted equivalent test loads caused by combined loading, J. Renew. Sustain. Energ., 12(1):013303, https://doi.org/10.1063/1.5112006,2020.

[15] Castro, O., Belloni, F., and Stolpe, M.: Optimized method for multi-axial fatigue testing of wind turbine blades, Compos. Struct, 257: 113358, https://doi.org/10.1016/j.compstruct.2020.113358, 2021.

[16] Melcher, D., Rosemann, H., and Haller, B.: Proof of concept: elliptical biaxial rotor blade fatigue test with resonant excitation, IOP Conf. Series: Mat. Sc. and Eng., 942(1): 012007, https://doi.org/10.1088/1757-899X/942/1/012007, 2020.

[17] Falko, B.: Biaxial Dynamic Fatigue Tests of Wind Turbine Blades, Ph.D. thesis, Leibniz University Hannover, Germany, https://publica.fraunhofer.de/handle/publica/283519, 2020.

Code and data availability.

The data that support the findings of this research are not publicly available due to confidentiality constraints.

Author contributions.

JS conceptualized and defined the requirements for the method developed. AZ supervised the work. JS and TD developed the model code and performed the simulations. JS prepared the manuscript with contributions from all co-authors.

Competing interests.

The authors declare that they have no conflict of interest.

Financial support.

Blade data of this research has been supported by Aeolon Technology Co., L